Structure Property Relationships: Asymmetric Oligofluorene−Thiophene Molecules for Organic TFTs

Ming L. Tang,[†] Mark E. Roberts,[‡] Jason J. Locklin,[‡] Mang M. Ling,[‡] Hong Meng,[§] and Zhenan Bao*[,‡]

Department of Chemistry and Department of Chemical Engineering, Stanford University, 381 North-South Mall, Stauffer III, Stanford, California 94305, and Central Research and Development, Experimental Station, E. I. DuPont Company, Wilmington, Delaware 19880-0328

Received October 2, 2006

Fluorene−thiophene oligomers show great promise as the active material in p-type organic thin film transistors (TFTs) because of their good performance and good stability under ambient conditions. In this study, a series of fluorene−thiophene co-oligomers were asymmetrically substituted with an alkyl group to probe the effect chemical structure has on their thin film properties. The alkyl groups are *n*-hexyl, *n*-octyl, and *n*-dodecyl, respectively. These oligomers were characterized by elemental analysis, mass spectrometry, differential scanning calorimetry, and thermogravimetric analysis, whereas the thin films of these oligomers were characterized by X-ray diffraction, atomic force microscopy, and field-effect transistor measurements. We found that the performance of these asymmetric molecules is similar to their symmetric counterparts. Mobilities as high as 0.16 $cm^2\ V^{-1}\ s^{-1}$ were found for the *n*-dodecyl-substituted oligomer.

Introduction

Organic semiconductors are the subject of intense research, because they have great potential in applications such as organic light-emitting diodes (OLEDs),[1−4] organic field-effect transistors (OFETs),[5−8] and photovoltaic cells.[9−13] Compared to current silicon-based technologies, organic semiconductors are amenable to large-area manufacturing. The use of flexible plastic substrates is also a possibility for organic semiconductors. Whereas the stability and reproducibility of OFETs fall short of that of amorphous silicon transistors, electronic circuits and displays powered by OFETs have been demonstrated.[14−17]

Materials that show promise for OFETs (field-effect mobilities, μ, greater than 0.1 $cm^2\ V^{-1}\ s^{-1}$ and on/off ratios, $I_{on/off}$, greater than 1×10^6 versus zero gate field) include oligoacenes such as pentacenes and oligothiophenes.[18−24] Almost all of these compounds are linear, symmetrically substituted molecules.

In this work, we designed a series of asymmetrically substituted conjugated molecules to study whether their morphology and field-effect mobility are any different from those of their symmetric counterparts, as the mechanism of growth of organic thin films by molecular vapor deposition is not well-understood. Prior to this, the only examples of asymmetric candidates for OFETs were the unsymmetrical 5-hexyl-2,2′;5′,2″;5″,2‴-quaterthiophene, and the 5″-benzo-[*b*]thiophen-2-yl-5-hexyl-[2,2′;5′,2″]terthiophene.[25] The authors found that the mobility of these molecules were on

* Corresponding author. E-mail: zbao@stanford.edu.
[†] Department of Chemistry, Stanford University.
[‡] Department of Chemical Engineering, Stanford University.
[§] E. I. Dupont Company.

(1) Chen, C. T. *Chem. Mater.* **2004**, *16*, 4389−4400.
(2) Friend, R. H.; Gymer, R. W.; Holmes, A. B.; Burroughes, J. H.; Marks, R. N.; Taliani, C.; Bradley, D. D. C.; Dos Santos, D. A.; Bredas, J. L.; Logdlund, M.; Salaneck, W. R. *Nature* **1999**, *397*, 121−128.
(3) Robinson, M. R.; Bazan, G. C.; Heeger, A. J.; O'Regan, M. B.; Wang, S. J. In *Molecules as Components of Electronic Devices*; Lieberman, M., Ed.; ACS Symposium Series 844; American Chemical Society: Washington, DC, 2003; pp 187−194.
(4) Forrest, S. R. *Nature* **2004**, *428*, 911−918.
(5) Newman, C. R.; Frisbie, C. D.; da Silva, D. A.; Bredas, J. L.; Ewbank, P. C.; Mann, K. R. *Chem. Mater.* **2004**, *16*, 4436−4451.
(6) Facchetti, A.; Yoon, M. H.; Marks, T. J. *Adv. Mater.* **2005**, *17*, 1705−1725.
(7) Ling, M. M.; Bao, Z. N. *Chem. Mater.* **2004**, *16*, 4824−4840.
(8) *Thin-Film Transistors*; Kagan, C. R., Andry, P. Eds.; CRC Press: Boca Raton, FL, 2003.
(9) Forrest, S. R. *MRS Bull.* **2005**, *30*, 28−32.
(10) Hagfeldt, A.; Gratzel, M. *Acc. Chem. Res.* **2000**, *33*, 269−277.
(11) Hoppe, H.; Sariciftci, N. S. *J. Mater. Res.* **2004**, *19*, 1924−1945.
(12) Schmidt-Mende, L.; Fechtenkotter, A.; Mullen, K.; Moons, E.; Friend, R. H.; MacKenzie, J. D. *Science* **2001**, *293*, 1119−1122.
(13) Yu, G.; Gao, J.; Hummelen, J. C.; Wudl, F.; Heeger, A. J. *Science* **1995**, *270*, 1789−1791.
(14) Klauk, H.; Gundlach, D. J.; Jackson, T. N. *IEEE Electron Device Lett.* **1999**, *20*, 289−291.
(15) Crone, B.; Dodabalapur, A.; Lin, Y. Y.; Filas, R. W.; Bao, Z.; LaDuca, A.; Sarpeshkar, R.; Katz, H. E.; Li, W. *Nature* **2000**, *403*, 521−523.
(16) Gelinck, G. H.; Huitema, H. E. A.; Van Veenendaal, E.; Cantatore, E.; Schrijnemakers, L.; Van der Putten, J.; Geuns, T. C. T.; Beenhakkers, M.; Giesbers, J. B.; Huisman, B. H.; Meijer, E. J.; Benito, E. M.; Touwslager, F. J.; Marsman, A. W.; Van Rens, B. J. E.; De Leeuw, D. M. *Nat. Mater.* **2004**, *3*, 106−110.
(17) Jackson, T. N.; Lin, Y. Y.; Gundlach, D. J.; Klauk, H. *IEEE J. Sel. Top. Quantum Electron.* **1998**, *4*, *100*.
(18) Kelley, T. W.; Baude, P. F.; Gerlach, C.; Ender, D. E.; Muyres, D.; Haase, M. A.; Vogel, D. E.; Theiss, S. D. *Chem. Mater.* **2004**, *16*, 4413−4422.
(19) Payne, M. M.; Parkin, S. R.; Anthony, J. E.; Kuo, C. C.; Jackson, T. N. *J. Am. Chem. Soc.* **2005**, *127*, 4986−4987.
(20) Garnier, F.; Horowitz, G.; Peng, X. H.; Fichou, D. *Adv. Mater.* **1990**, *2*, 592−594.
(21) Facchetti, A.; Letizia, J.; Yoon, M. H.; Mushrush, M.; Katz, H. E.; Marks, T. J. *Chem. Mater.* **2004**, *16*, 4715−4727.
(22) Meng, H.; Bendikov, M.; Mitchell, G.; Helgeson, R.; Wudl, F.; Bao, Z.; Siegrist, T.; Kloc, C.; Chen, C. H. *Adv. Mater.* **2003**, *15*, 1090−1093.
(23) Afzali, A.; Dimitrakopoulos, C. D.; Breen, T. L. *J. Am. Chem. Soc.* **2002**, *124*, 8812−8813.
(24) Katz, H. E.; Johnson, J.; Lovinger, A. J.; Li, W. J. *J. Am. Chem. Soc.* **2000**, *122*, 7787−7792.

10.1021/cm0623514 CCC: $33.50
Published on Web 12/19/2006

the same order of magnitude as the symmetric α,α′-dihexyl-quaterthiophene, and the α,α′-diBenzo[*b*]thiophen-2-nyl-bithiophene, respectively.

The fluorene−thiophene−fluorene conjugated core was chosen because it has a relatively low HOMO level of −5.36 eV. The molecules are stable for several months in ambient conditions.[26,27] Its HOMO level matches the work function of gold, allowing the injection of holes into the device. Charge mobilities as high as 0.12 and 0.16 $cm^2\ V^{-1}\ s^{-1}$ have been reported for the symmetrically substituted dihexyl and dicyclohexyl oligothiophene−fluorene TFTs, respectively.[26,28]

In this paper, we demonstrate that the mobility values of these asymmetric molecules are similar to their symmetric counterparts, especially for the molecules with longer alkyl substitutions. Interestingly, these asymmetric molecules seem to pack close to vertical on the substrate, compared to the symmetric molecules, which have a significant tilt angle.

Experimental Details

Instrumentation. Nuclear magnetic resonance (NMR) spectra was recorded on an Varian Inova-500 MHz spectrometer. Chemical shifts (δ) are reported in parts per million, and the residual solvent peak was used as an internal standard. The Philips PANalytical X'Pert diffractometer with a PreFIX X-ray mirror at the incident beam and a parallel plate collimator at the diffracted beam was used on the thin films of the evaporated molecules. $\omega/2\theta$ scans were performed with Cu Kα radiation at a power of 45 mV and 40 mA, with a step size of 0.02° and step time of 1.0 s. A Digital Instruments MMAFM-2 scanning probe microscope was used to perform tapping mode AFM on the samples with a silicon tip of 300 kHz frequency. Thermogravimetric analysis (TGA) was carried out on a Mettler Toledo TGA/SDTA851e thermogravimetric analyzer at a heating rate of 10 °C/min under a nitrogen flow rate of 75 cm^3/min. Differential scanning calorimetry (DSC) was performed on a TA Instruments Q100 V9.4 Build 287 DSC analyzer at a ramp rate of 10 °C/min under a nitrogen flow rate of 50 mL/min.

FET Device Fabrication. Top contact devices were made according to a literature procedure.[7,29] Dry thermally grown 300 nm silicon dioxide layer with a capacitance per unit area of 1.0×10^{-8} F/cm^2 functioned as the dielectric, whereas an *n*-doped silicon substrate functioned as the gate electrode. Shadow masks with *W*/*L* ratio of 20.75 ($W = 4000\ \mu m$, $L = 190\ \mu m$) were used after the evaporation of the organic semiconductor to deposit the gold drain and source electrodes. The organic semiconductors were deposited at a rate of 1 Å/s under a pressure of 6×10^{-6} mmHg to a final thickness of 45−50 nm, as determined by a quartz crystal monitor. TFT measurements were performed in air using a Keithley 4200 semiconductor parameter analyzer.

Synthesis. All chemical reagents were purchased from Aldrich Chemical Co., TCI, Lancaster, or Alfa Aesar and used as received. Solvents were purchased from Fisher.

5-(7-Hexyl-9H-fluoren-2-yl)-[2,2′]bithiophenyl (C6FTT). To a solution of 2-(7-hexyl-9H-fluoren-2-yl)-4,4,5,5-tetramethyl-1,3,2-dioxaboralane[26] (4.14 g, 0.011 mol) and 2-bromobithiophene (2.46 g, 0.010 mol) was added sodium carbonate (10.6 g, 0.10 mol) dissolved in water (50 mL) followed by the addition of phase-transfer agent Aliquat 336 (4 g, 0.010 mol). The mixture was bubbled with nitrogen for 15 min, after which tetrakis(triphenylphosphine)palladium(0) (0.8 g, 0.69 mmol) was added. The reaction mixture was heated to 80 °C for 16 h under a nitrogen atmosphere and then cooled to room temperature and quenched with methanol. The mixture was then filtered, washed with water, 5% $HCl_{(aq)}$, and water again. Upon drying, a bright yellow powder was collected (3.0 g, yield: 65%). ^{1}H NMR ($CDCl_3$, 500 MHz): δ_H 7.76 (d, $J = 1.0$ Hz, 1 H), 7.73 (d, $J = 8.0$ Hz, 1 H), 7.68 (d, $J = 7.5$ Hz, 1 H), 7.61 (dd, $J = 8.0$ Hz, 1.5 Hz, 1 H), 7.38 (s, 1 H), 7.26 (d, $J = 4.0$ Hz, 1 H), 7.23−7.20 (m, 3 H), 7.17 (d, $J = 4.0$ Hz, 1 H), 7.04 (dd, $J = 5.2$ Hz, 4.0 Hz, 1 H), 3.91 (s, 2 H), 2.68 (t, $J = 7.7$, 2H), 1.68−1.65 (m, 2 H), 1.39−1.30 (m, 6H), 0.89 (t, 3H). ^{13}C NMR ($CDCl_3$, 500 MHz): δ_C 144.18, 144.05, 143.91, 142.34, 141.74, 139.10, 137.83, 136.45, 132.32, 128.12, 127.46, 125.38, 124.90, 124.69, 124.51, 123.74, 123.57, 122.37, 120.17, 119.92, 37.05, 36.45, 32.06, 32.02, 29.31, 22.89, 14.38. Elemental Anal. Found: C, 78.01; H, 6.12; S, 15.26. Calcd for $C_{27}H_{26}S_2$: C, 78.21; H, 6.32; S, 15.47.

5-Bromo-5′-(7-hexyl-9H-fluoren-2-yl)-[2,2′]bithiophenyl (C6-FTTBr). 5-(7-Hexyl-9H-fluoren-2-yl)-[2,2′]bithiophenyl (0.64 g, 1.54 mmol) was dissolved in chloroform (25 mL) and cooled with an ice bath. Mercury acetate (0.98 g, 3.08 mmol) dissolved in acetic acid (10 mL) was added dropwise to the reaction mixture, followed by *N*-bromosuccinimide (NBS) (0.55 g, 3.08 mmol) dissolved in 10 mL of chloroform. The mixture was brought to room temperature, stirred for 3 h, quenched with H_2O, extracted with chloroform and dried with $MgSO_4$. Upon removal of solvent and recrystallization from chlorobenzene, a greenish yellow powder was isolated (0.85 g, yield: 85%). ^{1}H NMR ($CDCl_3$, 500 MHz): δ_H 7.74 (s, 1 H), 7.73 (d, $J = 7.5$ Hz, 1 H), 7.68 (d, $J = 7.5$ Hz, 1 H), 7.60 (d, $J = 7.5$ Hz, 1 H), 7.38 (s, 1 H), 7.24 (d, $J = 4.0$ Hz, 1 H), 7.20 (d, $J = 7.5$ Hz, 1 H), 7.09 (d, $J = 4.0$ Hz, 1 H), 6.99 (d, $J = 3.5$ Hz, 1 H), 6.94 (d, $J = 3.5$ Hz, 1 H), 3.91 (s, 2 H), 2.68 (t, $J = 8.0$, 2H), 1.67−1.63 (m, 2 H), 1.38−1.31 (m, 6H), 0.89 (t, 3H). ^{13}C NMR ($CDCl_3$, 500 MHz): δ_C 144.83, 144.21, 143.92, 142.41, 142.04, 139.44, 139.09, 135.40, 132.21, 130.88, 127.46, 125.29, 125.15, 124.83, 123.75, 123.56, 122.45, 120.12, 119.91, 111.05, 37.04, 36.40, 31.95, 31.83, 29.21, 22.77, 14.17. Elemental anal. Found: C, 65.71; H, 4.98; Br, 14.80; S, 12.39. Calcd for $C_{27}H_{25}BrS_2$: C, 65.71; H, 5.11; Br, 16.19; S, 12.99.

5-(9H-Fluoren-2-yl)-5′-(7-hexyl-9H-fluoren-2-yl)-[2,2′]bithiophenyl (C6FTTF). In a nitrogen-flushed two-necked flask was placed 5-bromo-5′-(7-hexyl-9H-fluoren-2-yl)-[2,2′]bithiophenyl (1.0 g, 2.03 mmol), 2-(9H-fluoren-2-yl)-4,4,5,5-tetramethyl-[1,3,2]dioxaborolane (0.6 g, 2.05 mmol), sodium carbonate (2.15 g, 20.3 mmol), Aliquat 336 (1.1 g, 2.7 mmol), water (25 mL), and toluene (15 mL). The mixture was bubbled with nitrogen for 15 min, after which tetrakis(triphenylphosphine)palladium(0) (0.12 g, 0.10 mmol) was added. The mixture was heated to 80 °C for 24 h under a nitrogen atmosphere, quenched with methanol, and filtered. The residue was washed with H_2O, 5% $HCl_{(aq)}$, H_2O, chloroform, and chlorobenzene, giving a yellow powder (0.94 g, yield: 81%). The product was further purified by sublimation under a high vacuum twice, to give 0.45 g of yellow powder (yield: 39%). MS (DEI) *m/z*: 578 (M^+) Elemental anal. Found: C, 82.98; H, 5.73; S, 10.88. Calcd for $C_{40}H_{34}S_2$: C, 83.00; H, 5.92; S, 11.08.

The following compounds have been synthesized using the same procedures as for the 2-hexyl-9H-fluorene.[26]

2-Octyl-9H-fluorene. White crystals (yield: 86%). ^{1}H NMR ($CDCl_3$, 500 MHz): δ_H 7.74 (d, $J = 7.5$ Hz, 1 H), 7.68 (d, $J = 8.0$

(25) Deman, A. L.; Tardy, J.; Nicolas, Y.; Blanchard, P.; Roncali, J. *Synth. Met.* **2004**, *146*, 365−371.
(26) Meng, H.; Zheng, J.; Lovinger, A. J.; Wang, B. C.; Van Patten, P. G.; Bao, Z. N. *Chem. Mater.* **2003**, *15*, 1778−1787.
(27) Meng, H.; Bao, Z. N.; Lovinger, A. J.; Wang, B. C.; Mujsce, A. M. *J. Am. Chem. Soc.* **2001**, *123*, 9214−9215.
(28) Locklin, J.; Li, D. W.; Mannsfeld, S. C. B.; Borkent, E. J.; Meng, H.; Advincula, R.; Bao, Z. *Chem. Mater.* **2005**, *17*, 3366−3374.
(29) Locklin, J.; Roberts, M. E.; Mannsfeld, S. C. B.; Bao, Z. *J. Macromol. Sci., Part C: Polym. Rev.* **2006**, *46*, 79−101.

Hz, 1 H), 7.51 (d, $J = 7.0$ Hz, 1 H), 7.36 (s, 1 H), 7.33 (d, $J = 7.0$ Hz, 1 H), 7.27 (dd, $J = 6.5$ Hz, 1.0 Hz, 1 H), 7.18 (d, $J = 8.0$ Hz, 1.0 H), 3.87 (s, 2 H), 2.67 (t, $J = 8.0$, 2H), 1.66−1.63 (m, 2 H), 1.35−1.26 (m, 10H), 0.89 (t, 3H). ^{13}C NMR ($CDCl_3$, 500 MHz): δ_C 145.41, 143.35, 142.62, 141.10, 138.55, 130.03, 128.41, 127.55, 125.35, 121.07, 120.14, 119.93, 36.89, 36.43, 32.16, 32.08, 29.76, 29.62, 29.52, 22.93, 14.39.

2-Dodecyl-9H-fluorene. White crystals (yield: 50%). ^{1}H NMR ($CDCl_3$, 500 MHz): δ_H 7.75 (d, $J = 7.5$ Hz, 1 H), 7.69 (d, $J = 8.0$ Hz, 1 H), 7.52 (d, $J = 7.0$ Hz, 1 H), 7.36 (s, 1 H), 7.34 (d, $J = 7.0$ Hz, 1 H), 7.27 (dd, $J = 6.5$ Hz, 1.0 Hz, 1 H), 7.19 (d, $J = 8.0$ Hz, 1.0 H), 3.87 (s, 2 H), 2.67 (t, $J = 8.0$, 2H), 1.67−1.64 (m, 2 H), 1.37−1.25 (m, 20H), 0.89 (t, 3H). ^{13}C NMR ($CDCl_3$, 500 MHz): δ_C 145.40, 143.36, 142.63, 141.09, 138.57, 130.04, 128.43, 127.54, 125.36, 121.06, 120.15, 119.94, 36.92, 36.46, 32.22, 32.10, 30.00, 29.98, 29.94, 29.91, 29.89, 29.84, 29.66, 22.99, 14.44.

The following compounds have been synthesized using the same procedures as for the 2-bromo-7-hexyl-9H-fluorene.[26]

2-Bromo-7-octyl-9H-fluorene. White crystals (yield: 86%). ^{1}H NMR ($CDCl_3$, 500 MHz): δ_H 7.65 (d, $J = 7.5$ Hz, 1 H), 7.64 (s, 1 H), 7.58 (d, $J = 8.0$ Hz, 1 H), 7.46 (dd, $J = 8.0$ Hz, 2.0 Hz, 1 H), 7.35 (s, 1 H), 7.19 (dd, $J = 8.0$ Hz, 0.5 Hz, 1 H), 3.85 (s, 2 H), 2.66 (t, $J = 8.0$, 2H), 1.66−1.63 (m, 2 H), 1.35−1.26 (m, 10H), 0.88 (t, 3H). ^{13}C NMR ($CDCl_3$, 500 MHz): δ_C 145.40, 143.35, 142.63, 141.08, 138.56, 130.04, 128.43, 127.54, 125.36, 121.06, 120.13, 119.94, 36.92, 36.44, 32.16, 32.09, 29.78, 29.64, 29.55, 22.96, 14.40.

2-Bromo-7-dodecyl-9H-fluorene. White crystals (yield: 70%). ^{1}H NMR ($CDCl_3$, 500 MHz): δ_H 7.64 (d, $J = 8.5$ Hz, 1 H), 7.64 (s, 1 H), 7.58 (d, $J = 8.0$ Hz, 1 H), 7.46 (dd, $J = 8.5$ Hz, 2.0 Hz, 1 H), 7.34 (s, 1 H), 7.19 (dd, $J = 7.25$ Hz, 0.5 Hz, 1 H), 3.84 (s, 2 H), 2.66 (t, $J = 7.5$, 2H), 1.66−1.63 (m, 2 H), 1.36−1.25 (m, 20H), 0.88 (t, 3H). ^{13}C NMR ($CDCl_3$, 500 MHz): δ_C 145.39, 143.33, 142.60, 141.08, 138.54, 130.02, 128.41, 127.53, 125.34, 121.04, 120.13, 119.93, 36.89, 36.45, 32.23, 32.10, 30.02, 29.98, 29.96, 29.91, 29.89, 29.84, 29.67, 23.00, 14.45.

The following compounds have been synthesized using the same procedures as that used for the 2-(7-hexyl-9H-fluoren-2-yl-4,4,5,5-tetramethyl-1,3,2-dioxaborolane.[26]

2-(7-Octyl-9H-fluoren-2-yl-4,4,5,5-tetramethyl-1,3,2-dioxaborolane. White crystals (yield: 54%). ^{1}H NMR ($CDCl_3$, 500 MHz): δ_H 7.97 (s, 1 H), 7.81 (d, $J = 7.5$ Hz, 1 H), 7.75 (d, $J = 7.5$ Hz, 1 H), 7.71 (d, $J = 8.0$ Hz, 1 H), 7.37 (s, 1 H), 7.19 (d, $J = 7.5$ Hz, 1 H), 3.86 (s, 2 H), 2.66 (t, $J = 8.0$, 2H), 1.66−1.63 (m, 2 H), 1.35−1.26 (m, 22H), 0.88 (t, 3H). ^{13}C NMR ($CDCl_3$, 500 MHz): δ_C 145.03, 144.44, 142.72, 142.66, 139.43, 133.66, 131.48, 127.38, 125.44, 120.38, 119.26, 83.99, 36.89, 36.51, 32.21, 32.14, 29.82, 29.69, 29.58, 25.20, 22.99, 14.44.

2-(7-Dodecyl-9H-fluoren-2-yl-4,4,5,5-tetramethyl-1,3,2-dioxaborolane. White crystals (yield: 47%). ^{1}H NMR ($CDCl_3$, 500 MHz): δ_H 7.97 (s, 1 H), 7.81 (d, $J = 8.0$ Hz, 1 H), 7.75 (d, $J = 8.0$ Hz, 1 H), 7.72 (d, $J = 7.5$ Hz, 1 H), 7.37 (s, 1 H), 7.20 (d, $J = 8.0$ Hz, 1 H), 3.86 (s, 2 H), 2.67 (t, $J = 7.5$, 2H), 1.66−1.63 (m, 2 H), 1.37−1.25 (m, 32H), 0.88 (t, 3H). ^{13}C NMR ($CDCl_3$, 500 MHz): δ_C 145.02, 144.43, 142.72, 142.65, 139.42, 133.65, 131.47, 127.36, 125.43, 120.37, 119.25, 83.98, 36.88, 36.50, 32.21, 32.14, 29.97, 29.94, 29.89, 29.84, 29.82, 29.69, 29.66, 25.20, 23.00, 14.44.

2-(9H-Fluoren-2-yl)-4,4,5,5-tetramethyl-[1,3,2]dioxaborolane. White crystals (yield: 50%). ^{1}H NMR ($CDCl_3$, 500 MHz): δ_H 8.01 (s, 1 H), 7.86−7.80 (m, 3 H), 7.56 (d, $J = 7.5$ Hz, 1 H), 7.39 (t, $J = 7.5$ Hz, 1 H), 7.33 (t, $J = 7.5$ Hz, 1 H), 3.91 (s, 2 H), 1.38 (s, 12H). ^{13}C NMR ($CDCl_3$, 500 MHz): δ_C 144.84, 144.17, 142.73, 141.78, 133.65, 131.54, 127.49, 127.02, 125.40, 120.65, 119.56, 84.04, 36.99, 25.18.

The following compounds have been synthesized using the same procedures as those used for the C6FTT.

C8FTT. Yellow crystals (yield: 72%). ^{1}H NMR ($CDCl_3$, 500 MHz): δ_H 7.76 (d, $J = 1.0$ Hz, 1 H), 7.73 (d, $J = 8.0$ Hz, 1 H), 7.68 (d, $J = 8.0$ Hz, 1 H), 7.61 (dd, $J = 8.0$ Hz, 2.0 Hz, 1 H), 7.37 (s, 1 H), 7.26 (d, $J = 4.0$ Hz, 1 H), 7.23−7.20 (m, 3 H), 7.16 (d, $J = 3.5$ Hz, 1 H), 7.04 (dd, $J = 5.0$ Hz, 3.5 Hz, 1 H), 3.91 (s, 2 H), 2.68 (t, $J = 8.0$, 2H), 1.67−1.63 (m, 2 H), 1.36−1.27 (m, 10H), 0.88 (t, 3H). ^{13}C NMR ($CDCl_3$, 500 MHz): δ_C 144.17, 144.05, 143.91, 142.34, 141.74, 139.10, 137.83, 136.45, 132.32, 128.12, 127.46, 125.37, 124.89, 124.68, 124.50, 123.73, 123.56, 122.36, 120.16, 119.92, 37.05, 36.46, 32.16, 32.10, 29.78, 29.65, 29.54, 22.94, 14.39. Elemental anal. Found: C, 78.41; H, 6.76; S, 12.23. Calcd for $C_{29}H_{30}S_2$: C, 78.68; H, 6.83; S, 14.49.

C12FTT. Yellow crystals (yield: 55%). ^{1}H NMR ($CDCl_3$, 500 MHz): δ_H 7.76 (d, $J = 1.0$ Hz, 1 H), 7.73 (d, $J = 8.0$ Hz, 1 H), 7.68 (d, $J = 8.0$ Hz, 1 H), 7.61 (dd, $J = 8.0$ Hz, 1.0 Hz, 1 H), 7.37 (s, 1 H), 7.26 (d, $J = 4.0$ Hz, 1 H), 7.23−7.20 (m, 3 H), 7.16 (d, $J = 3.5$ Hz, 1 H), 7.04 (dd, $J = 5.0$ Hz, 3.5 Hz, 1 H), 3.91 (s, 2 H), 2.68 (t, $J = 8.0$, 2H), 1.67−1.64 (m, 2 H), 1.36−1.25 (m, 20H), 0.88 (t, 3H). ^{13}C NMR ($CDCl_3$, 500 MHz): δ_C 144.17, 144.05, 143.91, 142.35, 141.74, 139.10, 137.83, 136.45, 132.32, 128.12, 127.46, 125.38, 124.89, 124.68, 124.51, 123.73, 123.56, 122.37, 120.16, 119.92, 37.05, 36.46, 32.18, 32.10, 29.94, 29.91, 29.89, 29.86, 29.81, 29.77, 29.62, 22.95, 14.39. Elemental anal. Found: C, 79.62; H, 7.91; S, 11.86. Calcd for $C_{33}H_{38}S_2$: C, 79.46; H, 7.68; S, 12.86.

The following compounds have been synthesized using the same procedures as for the C6FTTBr.

C8FTTBr. Greenish yellow powder (yield: 64%). ^{1}H NMR ($CDCl_3$, 500 MHz): δ_H 7.75 (s, 1 H), 7.73 (d, $J = 7.5$ Hz, 1 H), 7.68 (d, $J = 7.5$ Hz, 1 H), 7.60 (d, $J = 7.5$ Hz, 1 H), 7.39 (s, 1 H), 7.24 (d, $J = 4.0$ Hz, 1 H), 7.20 (d, $J = 7.5$ Hz, 1 H), 7.09 (d, $J = 4.0$ Hz, 1 H), 6.99 (d, $J = 3.5$ Hz, 1 H), 6.94 (d, $J = 3.5$ Hz, 1 H), 3.91 (s, 2 H), 2.68 (t, $J = 8.0$, 2H), 1.67−1.63 (m, 2 H), 1.38−1.31 (m, 10H), 0.89 (t, 3H). ^{13}C NMR ($CDCl_3$, 500 MHz): δ_C 144.82, 144.21, 143.91, 142.41, 142.03, 139.43, 139.09, 135.39, 132.20, 130.87, 127.45, 125.28, 125.14, 124.82, 123.74, 123.55, 122.45, 120.11, 119.89, 111.04, 37.04, 36.40, 32.08, 31.87, 29.68, 29.57, 29.43, 22.82, 14.16. Elemental anal. Found: C, 65.71; H, 4.98; Br, 14.80; S, 12.39. Calcd for $C_{29}H_{29}BrS_2$: C, 66.78; H, 5.60; Br, 15.32; S, 12.30.

C12FTTBr. Greenish yellow powder (yield: 75%). ^{1}H NMR ($CDCl_3$, 500 MHz): δ_H 7.74 (s, 1 H), 7.73 (d, $J = 8.5$ Hz, 1 H), 7.68 (d, $J = 7.5$ Hz, 1 H), 7.60 (d, $J = 8.0$ Hz, 1 H), 7.37 (s, 1 H), 7.24 (d, $J = 4.0$ Hz, 1 H), 7.20 (d, $J = 7.5$ Hz, 1 H), 7.09 (d, $J = 4.0$ Hz, 1 H), 6.99 (d, $J = 3.5$ Hz, 1 H), 6.94 (d, $J = 3.5$ Hz, 1 H), 3.91 (s, 2 H), 2.68 (t, $J = 8.0$, 2H), 1.67−1.64 (m, 2 H), 1.33−1.26 (m, 20H), 0.88 (t, 3H). ^{13}C NMR ($CDCl_3$, 500 MHz): δ_C 144.82, 144.21, 143.91, 142.42, 142.04, 139.43, 139.09, 135.39, 132.21, 130.87, 127.45, 125.29, 125.14, 124.83, 123.74, 123.55, 122.45, 120.11, 119.90, 111.04, 37.04, 36.40, 32.10, 31.86, 29.84, 29.81, 29.78, 29.75, 29.72, 29.56, 29.51, 22.84, 14.18. Elemental anal. Found: C, 67.70; H, 6.84; Br, 10.31; S, 9.30. Calcd for $C_{33}H_{37}BrS_2$: C, 68.61; H, 6.46; Br, 13.83; S, 11.10.

The following compounds have been synthesized using the same procedures as for the C6FTTF.

C8FTTF. Orange powder (yield: 40%). MS (DEI) *m/z*: 606 (M^+) Elemental anal. Found: C, 82.90; H, 6.19; S, 10.53. Calcd for $C_{42}H_{38}S_2$: C, 83.12; H, 6.31; S, 10.57.

C12FTTF. Yellow powder (yield: 45%). MS (DEI) *m/z*: 662 (M^+) Elemental anal. Found: C, 83.59; H, 6.77; S, 9.40. Calcd for $C_{46}H_{46}S_2$: C, 83.33; H, 6.99; S, 9.67.

Scheme 1. Synthetic Route to Asymmetric Oligofluorene−Thiophene Molecules[a]

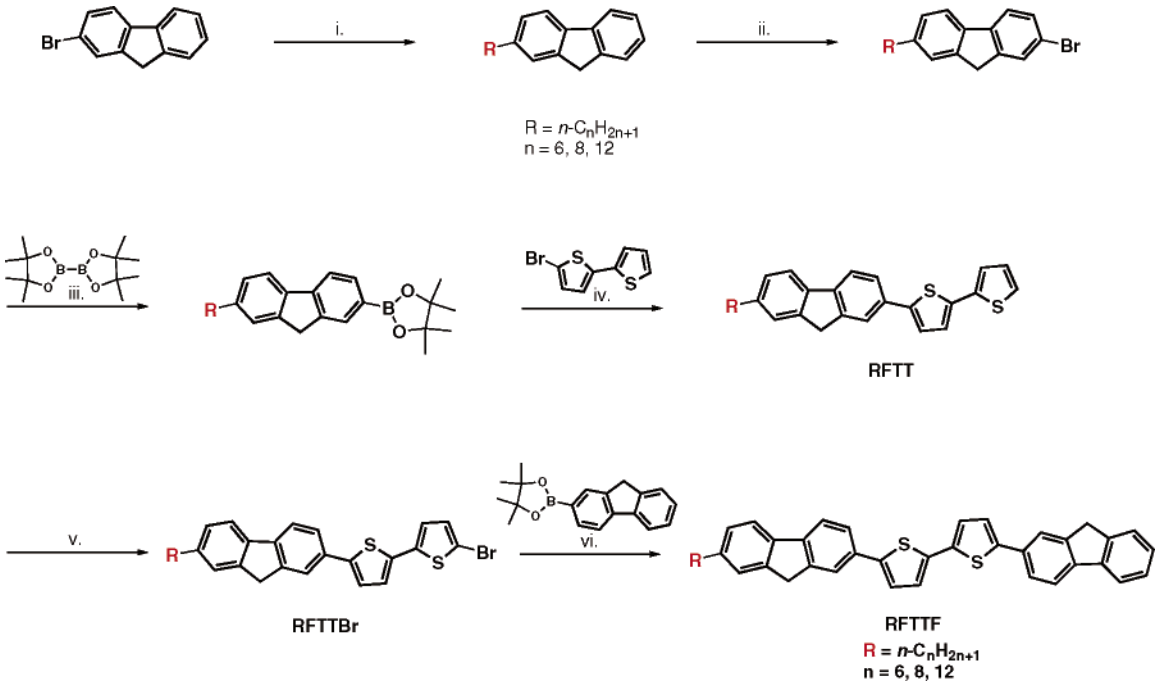

Results and Discussion

Synthesis. The synthesis of these asymmetric oligofluorene−thiophene molecules involved Kumada and Suzuki coupling reactions,[30] as shown in Scheme 1. First, the commercially available 2-bromo-9H-fluorene was added to the appropriate *n*-alkylmagnesium bromide under Kumada coupling conditions. The resulting product was then brominated and functionalized with a dioxaboralane to allow for Suzuki coupling with 2-bromobithiophene.[26] It should be noted that the 5-(7-alkyl-9*H*-fluoren-2-yl)-[2,2′]bithiophenyl (*n*-alkylFTT) was easily dibrominated under normal bromination conditions, for example, with *N*-bromosuccinimide (NBS) in dimethylformamide. The addition of mercury acetate was found to give the intended monobrominated precursor (*n*-alkylFTTFBr). The reaction may proceed via an electrophilic bromoacetate intermediate and a mercury acetate bromide salt, which prevents dibromination.[31] This precursor was then coupled with 2-(9*H*-Fluoren-2-yl)-4,4,5,5-tetramethyl-[1,3,2]dioxaborolane to give the desired product (*n*-alkylFTTF), which is quite insoluble in common solvents. Each oligomer was purified twice by temperature-gradient sublimation in a three-zone furnace under high vacuum at $\sim 1 \times 10^{-6}$ Torr to remove residual catalyst and other impurities, yielding yellow-orange powders.

All the intermediate precursors have been characterized by elemental analysis, ^{1}H, and ^{13}C NMR, whereas the final products have been characterized by elemental analysis and mass spectrometry. The results are consistent with the predicted chemical structures.

Thermal Properties. Thermogravimetric analysis (TGA) reveals that the asymmetric *n*-alkyl oligofluorene−thiophene oligomers (*n*-alkylFTTF) are thermally stable, with the onset of decomposition at 410 °C under a nitrogen atmosphere. Differential scanning calorimetry (DSC) gives the major endothermic melting peaks for *n*-hexylFTTF (C6FTTF), *n*-octylFTTF (C8FTTF), and *n*-dodecylFTTF (C12FTTF) as 390, 387, and 384 °C, respectively, and the corresponding major exothermic crystallization peaks as 386, 384, and 381 °C, respectively. Figure 1 illustrates the heating and cooling process for the oligomers.

X-ray Diffraction. X-ray diffraction of the C6FTTF oligomer showed two peaks of $n = 2$ and 4; that of the C8FTTF oligomer showed three peaks of $n = 2$, 4, and 8; and that of the C12FTTF oligomer showed five peaks of $n = 3$, 4, 5, 6, and 9. The assigned indice is an integer that would multiply the corresponding *d*-spacing to give the approximate molecular length. Although it is rare to see a ninth order peak in a thin film of organic material, Garnier et al.[32] report up to 34 orders of diffraction in micrometer-thick evaporated films of α,ω-dihexylsexithiophene. The noisy background observed in the X-ray diffraction patterns is due to the 50 nm thin films being only 10−14 molecular layers thick. From all the measurements of each oligomer at

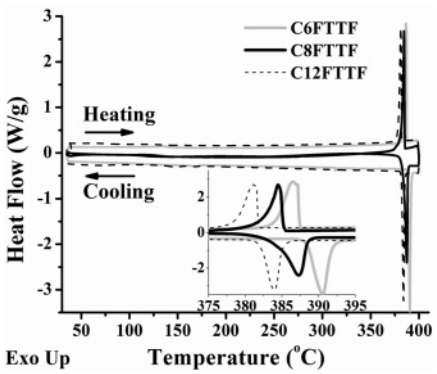

Figure 1. Differential scanning calorimetry (DSC) thermograms of the oligomers. Positive heat flow corresponds to an exothermic transition.

(30) Ohe, T.; Miyaura, N.; Suzuki, A. *J. Org. Chem.* **1993**, *58*, 2201−2208.
(31) Hatanaka, Y.; Keefer, R. M.; Andrews, L. J. *J. Am. Chem. Soc.* **1965**, *87*, 4280−4285.

Table 1. Average *d*-Spacings and Calculated Molecular Lengths of the Asymmetric *n*-alkylFTTF Molecules.

	X-ray diffraction data							
molecule	*T* (°C)	surface	2θ (deg)	average *d*-spacing (Å)	order (*n*)	net height	unit cell constant (Å)	MM2 minimized length (Å)
C6FTTF	100	OTS/SiO_2/Si	5.57	15.86	2	3482	31.4 ± 0.4	31.79
			11.35	7.78	4	899		
	140	SiO_2/Si	5.62	15.72	2	1924	31.6 ± 0.3	
			11.11	7.96	4	611		
		OTS/SiO_2/Si	5.48	16.11	2	902	31.9 ± 0.4	
			11.14	7.93	4	399		
C8FTTF	100	OTS/SiO_2/Si	5.29	16.69	2	2054	33.2 ± 0.2	34.08
			10.68	8.27	4	1885		
	140	SiO_2/Si	5.21	16.96	2	17664	33.7 ± 0.2	
			10.50	8.42	4	5419		
			21.17	4.19	8	774		
		OTS/SiO_2/Si	5.26	16.70	2	810	33.4 ± 0.1	
			10.61	8.33	4	1148		
			21.10	4.20	8	250		
C12FTTF	100	OTS/SiO_2/Si	7.21	12.25	3	1563	36.8 ± 0.2	38.34
			9.62	9.19	4	1945		
			12.04	7.35	5	715		
			14.54	6.08	6	434		
			21.54	4.12	9	425		
	140	SiO_2/Si	7.09	12.45	3	703	37.9 ± 0.4	
			9.26	9.55	4	698		
			11.47	7.68	5	175		
			14.13	6.25	6	440		
			21.07	4.21	9	382		
		OTS/SiO_2/Si	7.00	12.53	3	1132	37.9 ± 0.2	
			9.30	9.52	4	1004		
			11.59	7.63	5	535		
			13.96	6.33	6	372		
			21.11	4.20	9	506		

different conditions (each deposited at a substrate temperature of 100 and 140 °C, on either bare SiO_2 substrates or on SiO_2 substrate treated with OTS), we find that the average *d*-spacing for the C6FTTF is 31.6 Å with a standard deviation of 0.2 Å; for the C8FTTF, it is 33.6 Å with a standard deviation of 0.1 Å; and for the C12FTTF oligomer, it is 37.5 Å with a 0.2 Å standard deviation. The 2θ values and the respective *d*-spacings of the *n*-alkylFTTF at a given deposition condition are given in Table 1. The low standard deviations indicate that the molecular orientation of the oligomers changed very little with varying substrate surface and temperature.

The observed *d*-spacings are consistent with layers that are one molecular layer thick, with an increase in *d*-spacing of an average of 0.96 Å for each methylene unit. The molecules appear to be packed edge-on on the substrate, with tilt angles less than 10°, based on the MM2 energy-minimized lengths of C6FTTF, C8FTTF, and C12FTTF being 31.79, 34.08, and 38.34 Å, respectively, in contrast to the symmetrical cyclohexyl-disubstituted oligothiophene−fluorene oligomer, which has a tilt angle of 20°,[28] and the dihexyl-substituted molecule, which has a tilt angle of 30°.[26] The unsubstituted FTTF molecule has a tilt angle of 17°[27] in between the symmetric and asymmetric FTTF molecules, which may explain its optimized mobility being an order of magnitude lower than the alkyl-substituted molecules. Though the MM2 calculated length of the asymmetric *n*-alkylFTTF is almost equal to the observed *d*-spacing, it does not take into account the interlayer spacing due to van der Waals forces. Qualitatively, it can be seen that the asymmetric FTTF molecules tilt less than the symmetric dialkylated FTTF because there is one less alkyl unit for tilt to be introduced. This is because in a close-packed film, the distance between the conjugated cores of adjacent molecules is less than the distance between the alkyl chains, resulting in an angle between the conjugated core and the alkyl chain.[32]

For all the *n*-alkylFTTFs, additional peaks of higher order are observed only on films grown at a substrate temperature of 100 and 140 °C. This implies that the films are more crystalline at higher substrate temperature during deposition.

Morphology. Figures 2−4 show AFM height images of 50 nm thick films of the oligomers deposited on both OTS-treated SiO_2/Si or plain SiO_2/Si at room temperature and 100 and 140 °C, respectively. Similar morphology is observed on both substrates at a substrate deposition temperature of 20 °C. At this temperature, the films are made of small, irregular grains ranging from 100−300 nm in length. The films are very uneven, with regions of extreme altitude occurring randomly. At 100 °C, bigger grains of roughly 2 μm are seen for all the oligomers. The molecules become more ordered, and a network of interconnected grains can be observed for the C8FTTF sample. At 140 °C, large grains, some as big as 12 μm, are seen on both bare SiO_2/Si substrates and OTS-treated substrates for all the molecules. The molecules seem to pack edge-on, as suggested by the measured terrace heights measured by AFM. These terraced grains have clear facets, and their interconnected nature accounts for the high mobility observed at this temperature. The AFM step heights for the C6FTTF, C8FTTF, and C12FTTF molecules as obtained from the films deposited at 140 °C are 29, 30, and 38 Å, respectively, corresponding well with the *d*-spacing obtained from X-ray and the calculated molecular length.

(32) Gamier, F.; Yassar, A.; Hajlaoui, R.; Horowitz, G.; Deloffre, F.; Serve, B.; Ries, S.; Alnott, P. *J. Am. Chem. Soc.* **1993**, *115*, 8716−8712.

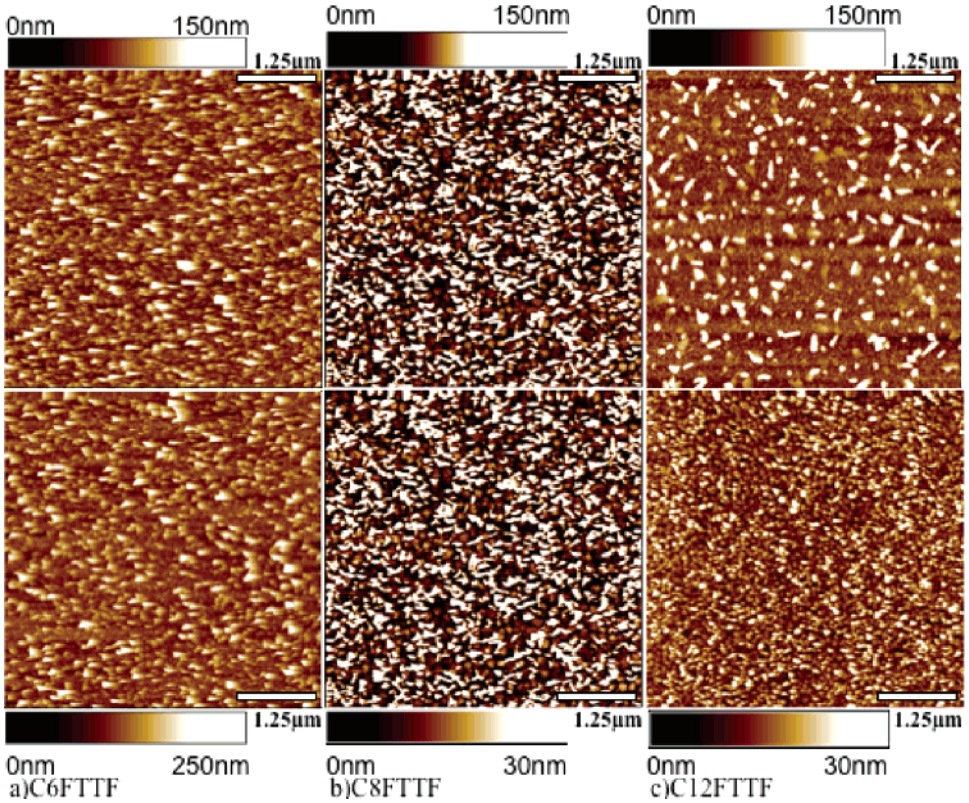

Figure 2. AFM height images of 50 nm *n*-alkylFTTF films deposited onto SiO_2/Si (top row) and OTS/SiO_2/Si (bottom row) at room temperature. Each image is 5 × 5 μm.

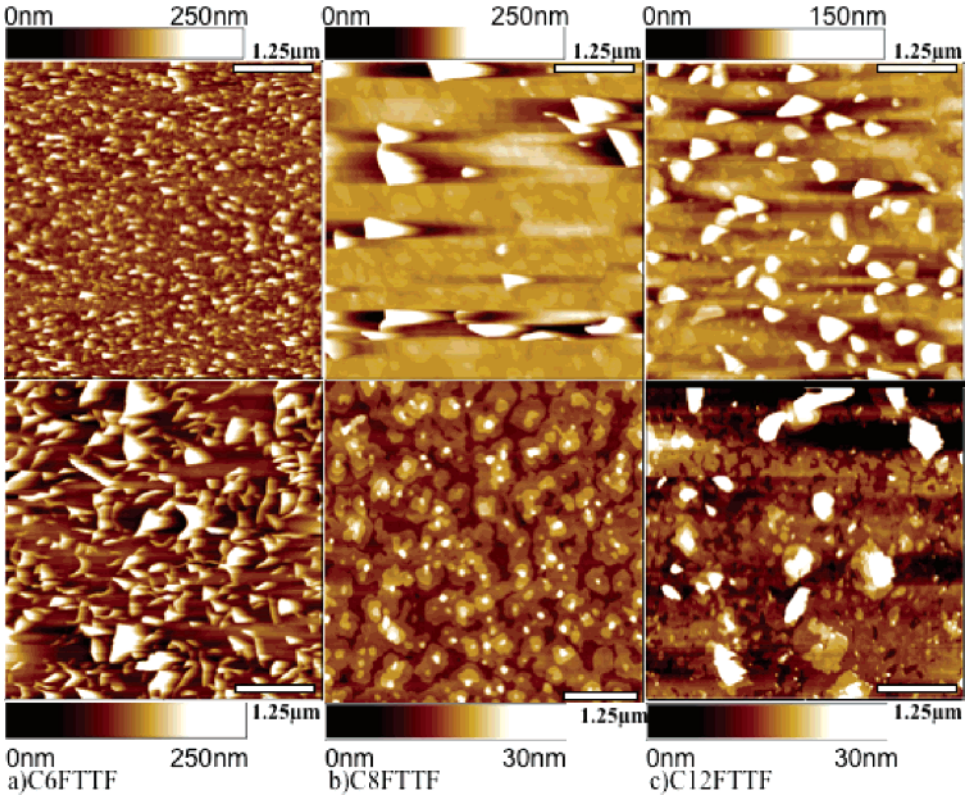

Figure 3. AFM height images of 50 nm *n*-alkylFTTF films deposited onto SiO_2/Si (top row) and OTS/SiO_2/Si (bottom row) at 100 °C substrate temperature. Each image is 5 × 5 μm.

At room temperature, the oligomers tend to grow in the island mode (Volmer−Weber mode[33]), but at high temperature, they grow in the layer-by-layer mode (Frank−van der Merwe mode[33]). In inorganic films, the island mode occurs when the atoms prefer to interact with themselves rather than the substrate, whereas the layer-by-layer mode occurs when atoms prefer to bind to the substrate rather than themselves.[34] Similarly, conjugated organic molecules prefer to associate

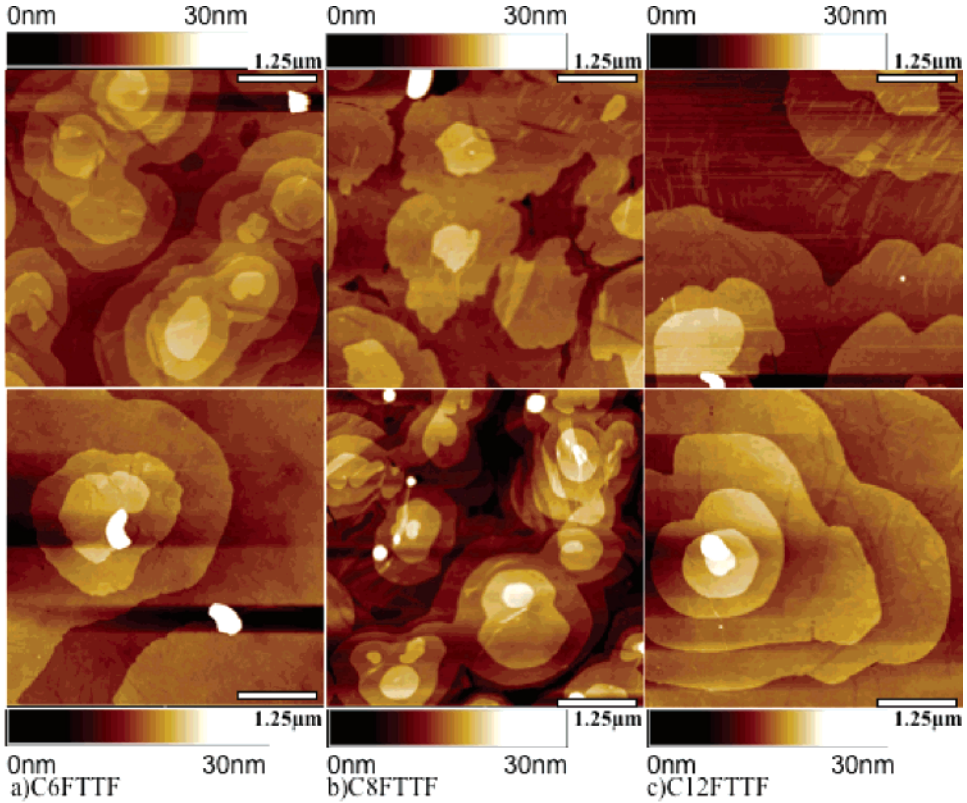

Figure 4. AFM height images of 50 nm *n*-alkylFTTF films deposited onto SiO_2/Si (top row) and OTS/SiO_2/Si (bottom row) at a 140 °C substrate temperature. Each image is 5 × 5 μm.

Table 2. Average Field-Effect Mobilities over 5 Devices, μ(cm^2 V^{-1} s^{-1}), On/Off Ratios, $I_{on/off}$, and Threshold Voltages (V) for C6FTTF, C8FTTF, and C12FTTF (W/L = 20) at Three Substrate Temperatures, T_{sub}(°C) on Bare and OTS-Treated Silicon Dioxide

surface		C6FTTF	C8FTTF	C12FTTF	T_{sub} (°C)
SiO_2/Si	μ	0.018 ± 0.0003	0.016 ± 0.0005	0.0066 ± 0.001	20
	I_{on}/I_{off}	6×10^3	2×10^5	1×10^5	
	V_T	−16	−27	−28	
OTS/SiO_2/Si	μ	0.030 ± 0.0007	0.028 ± 0.0002	0.036 ± 0.001	
	I_{on}/I_{off}	9×10^4	5×10^5	2×10^6	
	V_T	−16	−16	−21	
SiO_2/Si	μ	0.020 ± 0.0001	0.031 ± 0.0007	0.073 ± 0.004	100
	I_{on}/I_{off}	6×10^4	5×10^3	4×10^4	
	V_T	−3	−4	−10	
OTS/SiO_2/Si	μ	0.099 ± 0.001	0.092 ± 0.001	0.12 ± 0.002	
	I_{on}/I_{off}	6×10^4	1×10^6	2×10^6	
	V_T	−2	−8	−10	
SiO_2/Si	μ	0.051 ± 0.002	0.050 ± 0.0006	0.093 ± 0.003	140
	I_{on}/I_{off}	2×10^4	2×10^4	5×10^5	
	V_T	1	−6	−4	
OTS/SiO_2/Si	μ	0.097 ± 0.0004	0.10 ± 0.001	0.15 ± 0.009	
	I_{on}/I_{off}	4×10^5	2×10^6	2×10^6	
	V_T	−4	−8	−7	

with each other at room temperature, forming small islands on the substrate, but at higher substrate temperature, they have enough energy to diffuse around to form thermodynamically favorable layers, leading to layer-by-layer growth. At higher temperatures, there exists a lower energy barrier to the aggregation of a critical number of molecules required for nucleation for layer-by-layer growth.[35]

FET Device Performance. Table 2 shows the field-effect mobility for the three oligomers. The TFTs were made by sublimating the molecules onto a 300 nm thick SiO_2 dielectric thermally grown on highly doped silicon, which served as a gate electrode. TFTs were also made on OTS-modified SiO_2/Si substrates. Gold was deposited using shadow masks, which made source and drain electrodes with $W/L = 20.75$. The field-effect mobility, μ, was extracted from transfer curves using eq 1, where I_{DS} is the drain-source current in the saturated regime, W/L the ratio of the channel width to the channel length of the organic semiconductor, C_i the capacitance of the SiO_2 dielectric layer, V_G the gate voltage, and V_T the threshold voltage.

$$I_{DS} = \frac{WC_i\mu}{2L}(V_G - V_T)^2$$

The best μ values for the C6FTTF, C8FTTF, and C12FTTF

(33) Venables, J. A.; Spiller, G. D. T.; Hanbucken, M. *Rep. Prog. Phys.* **1984**, *47*, 399−459.
(34) Ruiz, R.; Choudhary, D.; Nickel, B.; Toccoli, T.; Chang, K. C.; Mayer, A. C.; Clancy, P.; Blakely, J. M.; Headrick, R. L.; Iannotta, S.; Malliaras, G. G. *Chem. Mater.* **2004**, *16*, 4497−4508.
(35) Verlaak, S.; Steudel, S.; Heremans, P.; Janssen, D.; Deleuze, M. S. *Phys. Rev. B* **2003**, *68*.

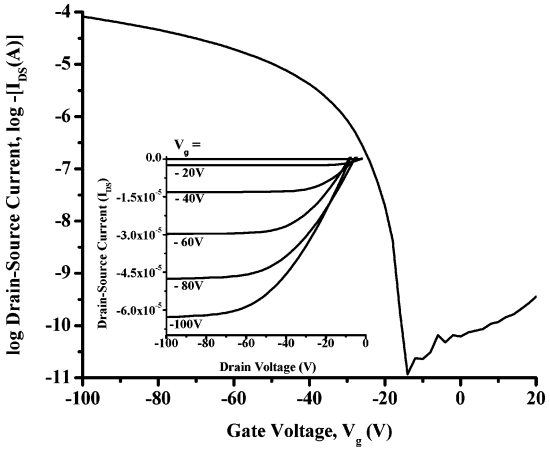

Figure 5. Characteristic output and transfer TFT curves for 50 nm C12FTTF deposited on OTS treated SiO_2/Si at $T_{sub} = 140$ °C. This curve is representative of all devices measured.

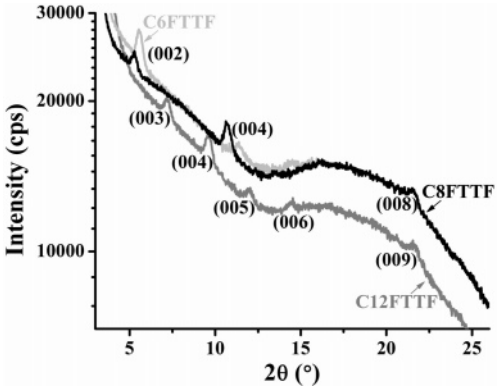

Figure 6. X-ray diffractograms of 50 nm evaporated thin films of the oligomers on OTS-treated substrates at a deposition temperature of 100 °C.

were obtained on OTS-treated SiO_2/Si at $T_{sub} = 140$ °C; the values were 0.098, 0.103, and 0.161 $cm^2\ V^{--}\ s^{-1}$, respectively, on the same order of magnitude as the unsubstitued, hexyl, and cyclohexyl-disubstitued FTTF molecules.[26,28] A characteristic output and transfer curve for a device is shown in Figure 5.

The mobility trends correlate well with the thin film morphology observed. Higher mobility is observed when the thin films have smoother grains, larger grain size, and higher crystallinity.

A high aspect ratio in a molecule reduces the cohesion force between adjacent molecular layers,[35] but increases the energy barrier required for nucleation. Both these factors promote layer-by-layer growth, as opposed to island growth. As expected, the C12FTTF, with a higher aspect ratio than C6FTTF and C8FTTF, displays larger grains at 140 °C (as seen in the AFM images), more orders of diffraction in X-ray scans (Figure 2 and Table 1), and correspondingly higher mobility values. However, the grain size of the oligomers appear similar for films deposited at room temperature and 100 °C, with the C12FTTF displaying smaller grains and a lower mobility than the shorter oligomers at room temperature. This can be attributed to the fact that a larger amount of kinetic or thermal energy is required for a larger molecule to diffuse to a thermodynamically more stable site on the substrate; otherwise, a less-ordered film with small grains is formed. Such films have more grain boundaries, which lower the mobility of polycrystalline organic thin films, as charge transport is limited by these boundaries.[36] More detailed studies on the growth behavior of these molecules and their symmetric counterparts are underway.

Conclusion

The TFT characteristics of asymmetric *n*-alkyl oligofluorene−thiophene molecules are as high as their symmetric counterparts. At high temperatures, the longer the alkyl group, the more ordered the thin film. In contrast to their symmetrical counterparts that pack with their long axis at a tilt angle to the substrate, they pack close to perpendicular to the substrate. They also have much larger grains than the symmetric oligomers as shown by AFM. This means that the linear alkyl groups, which do not contribute to charge transport but contribute to order in the polycrystalline grains, are not required in a symmetric manner. Perhaps the asymmetrically substituted versions of other conjugated small molecules might outperform their symmetric counterparts, when the correct ratio of the conjugated core to the nonconjugated segment is found.

Acknowledgment. M.L.T. thanks Stefan Mannsfeld, Randy Stoltenberg, and Wei You for helpful suggestions and discussions. She acknowledges a Kodak graduate fellowship. Z.B. acknowledges partial financial support from a Dupont Science and Technology Grant, the Stanford Center for Polymer Interfaces and Macromolecular Assemblies (NSF Center MRSEC under Award DMR-0213618), and a 3M Faculty Award.

CM0623514

(36) Horowitz, G.; Hajlaoui, M. E. *Adv. Mater.* **2000**, *12*, 1046−1050.